JACS
JOURNAL OF THE AMERICAN CHEMICAL SOCIETY
Communication
pubs.acs.org/JACS

Tuning of Photoluminescence by Cation Nanosegregation in the $(CaMg)_x(NaSc)_{1-x}Si_2O_6$ Solid Solution

Zhiguo Xia,[*,†] Guokui Liu,[*,‡] Jianguo Wen,[§] Zhigang Mei,[∥] Mahalingam Balasubramanian,[⊥] Maxim S. Molokeev,[#,▽] Licong Peng,[○] Lin Gu,[○] Dean J. Miller,[§] Quanlin Liu,[†] and Kenneth R. Poeppelmeier[*,◆]

[†]The Beijing Municipal Key Laboratory of New Energy Materials and Technologies, School of Materials Sciences and Engineering, University of Science and Technology Beijing, Beijing 100083, China

[‡]Chemical Sciences and Engineering Division, [§]Center for Nanoscale Materials, Nanoscience and Technology Division, [∥]Nuclear Engineering Division, and [⊥]X-ray Science Division, Argonne National Laboratory, Argonne, Illinois 60439, United States

[#]Laboratory of Crystal Physics, Kirensky Institute of Physics, SB RAS, Krasnoyarsk 660036, Russia

[▽]Department of Physics, Far Eastern State Transport University, Khabarovsk 680021, Russia

[○]Beijing National Laboratory for Condensed Matter Physics, Institute of Physics, Chinese Academy of Sciences, Beijing 100190, China

[◆]Department of Chemistry, Northwestern University, 2145 Sheridan Road, Evanston, Illinois 60208, United States

Supporting Information

ABSTRACT: Controlled photoluminescence tuning is important for the optimization and modification of phosphor materials. Herein we report an isostructural solid solution of $(CaMg)_x(NaSc)_{1-x}Si_2O_6$ $(0 < x < 1)$ in which cation nanosegregation leads to the presence of two dilute Eu^{2+} centers. The distinct nanodomains of isostructural $(CaMg)Si_2O_6$ and $(NaSc)Si_2O_6$ contain a proportional number of Eu^{2+} ions with unique, independent spectroscopic signatures. Density functional theory calculations provided a theoretical understanding of the nanosegregation and indicated that the homogeneous solid solution is energetically unstable. It is shown that nanosegregation allows predictive control of color rendering and therefore provides a new method of phosphor development.

Rare-earth (RE)-activated inorganic phosphors have superb chemical and optical advantages in many applications.[1,2] Accordingly, RE luminescence tuning is highly desired for phosphor development. However, chemical modification of host materials leads to shifts of the absorption and emission energies and changes in transition intensities.[3,4] That is, when the structural and electronic alterations are induced locally in a random manner, the energy levels of the optical center shift, and tuning of the spectral profile is achieved through the creation of anisotropic local environments for the emitting RE ions; this is known as inhomogeneous broadening.[5] However, a recent study suggests that a different type of spectral tailoring can be achieved. Two emission bands from an isostructural solid solution of $(Ca_xNa_{1-x})(Mg_xSc_{1-x})Si_2O_6:Eu^{2+}$ were observed to be largely independent of composition variation.[6] The overall emission profile could be interpreted as a linear superposition of two bands from Eu^{2+} in the compounds $(CaMg)Si_2O_6$ (CMS) and $(NaSc)Si_2O_6$ (NSS). Initial structure characterization suggested that the studied materials formed a solid solution wherein the chemical constituents were homogeneously mixed. Jervisite, a scandium-containing mineral, is a sodic pyroxene that is intermediate in the $Ca(Mg,Fe)Si_2O_6$–$NaScSi_2O_6$ series and isostructural with the synthetic phase $NaScSi_2O_6$.[7,8] Spinodal decomposition across many pyroxene joins is known.[9,10]

Segregation usually involves the separation of materials into regions of different chemical compositions, and different types of segregation have been identified: phase, surface, dopant, defect, sublattice domain, and so on.[11,12] The spectroscopic characteristics of Eu^{2+} in $(NaSc)_x(CaMg)_{1-x}Si_2O_6$ can also be well-understood if cation segregation leads to the formation of nanoscale CMS and NSS domains based on the electronic properties of RE in crystalline solids as defined in crystal field theory and the Förster–Dexter theory of energy transfer.[5,13−15] Here the observed phenomenon arises from segregation of cation pairs of $(CaMg)^{4+}$ and $(NaSc)^{4+}$ at the nanometer scale without long-range structural discontinuity. Furthermore, the distance dependence of the ion–ligand electrostatic interactions and the Eu^{2+}–Eu^{2+} energy transfer allows us to estimate the size of the segregated domains. Optical spectroscopy, extended X-ray absorption fine structure (EXAFS), and aberration-corrected scanning transmission electron microscopy (STEM) were the primary experimental probes that allowed us to unequivocally identify the intrinsic nanosegregation in this system.

The emission spectra of $(CMS)_x(NSS)_{1-x}$:3%Eu^{2+} for x = 0.1–0.8 are largely composed of two distinct emission bands, each of which is identifiably present in the end compounds (x = 0, 1) (Figure 1a). The spectra of $(CMS)_x(NSS)_{1-x}$:3%Eu^{2+} were quantitatively fitted with the linear function

$$I(x') = C[x'I(\mathrm{CMS}) + (1 - x')I(\mathrm{NSS})] \quad (1)$$

Received: December 7, 2015
Published: January 15, 2016

DOI: 10.1021/jacs.5b12788
J. Am. Chem. Soc. 2016, 138, 1158–1161

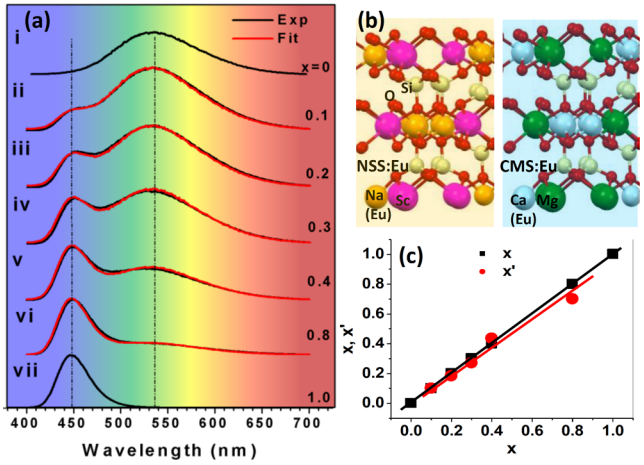

Figure 1. (a) Photoluminescence emission spectra of $(CMS)_x(NSS)_{1-x}:Eu^{2+}$ as a function of x. The experimental spectra for $0 < x < 1$ were fit with the linear combination $x'I(CMS) + (1 - x')I(NSS)$ based on the pure-phase spectra $I(NSS)$ and $I(CMS)$, plotted as (i) and (vii), respectively. (b) Atomic structures of NSS:Eu and CMS:Eu. (c) Values of x' determined from the fitting plotted vs x for (ii) $x' = 0.1$, (iii) $x' = 0.183$, (iv) $x' = 0.27$, (v) $x' = 0.435$, and (vi) $x' = 0.7$.

where $I(NSS)$ and $I(CMS)$ are the intensities of the experimental spectra of NSS:3%Eu^{2+} and CMS:3%Eu^{2+} plotted in Figure 1a(i,vii) and C and x' are constants adjusted to fit the individual experimental spectra for different values of x. The fitted values x' are very close to the x values, i.e., the (CaMg):(NaSc) composition ratios in the samples. Moreover, the emission wavelength center, bandwidth, and spectral profile are all invariant from those of Eu^{2+} in the end compounds. It is therefore very clear that the luminescence from the solid solution is produced from a linear superposition of the emissions of the two end compounds, which thus provides evidence that Eu^{2+} ions have chemical and electronic environments similar to those found in the single-phase end compounds. As marked by the dotted vertical lines in Figure 1a, the emission centers and full width at half-maximum (fwhm) values remain invariant, with a narrow blue band peaking at 449 nm (fwhm = 36 nm) and a broad yellow band centered at 532 nm (fwhm = 120 nm).

The optical spectroscopy study revealed that the $(CMS)_x(NSS)_{1-x}:Eu^{2+}$ solid solution gives rise to the same spectra as that of the physically mixed bulk phosphors of CMS:Eu^{2+} and NSS:Eu^{2+}. This strongly implies that chemical segregation occurs and leads to the formation of domains similar to the pure phases of CMS:Eu^{2+} and NSS:Eu^{2+}. Details of the thermal quenching behavior of both emission bands, the luminescence decay dynamics, and theoretical modeling are discussed in the Supporting Information (SI 1). In addition to the photoluminescence spectra, the dynamics of the luminescence decay of Eu^{2+} in the $(CMS)_x(NSS)_{1-x}:Eu^{2+}$ solid solution indicates that energy transfer occurs exclusively among the Eu^{2+} ions within the domains with no exchange between the CMS and NSS domains. Because energy transfer is induced by the Eu^{2+}–Eu^{2+} interaction, which depends on the distance between the two Eu^{2+} ions (donor and acceptor), the absence of energy transfer between the domains implies that the two different Eu^{2+} emitting centers are separated far enough from each other and do not interact.[16,17] This observation is consistent with the spectroscopic results discussed above and reinforces the conclusion that the unusual spectroscopic properties of $(CMS)_x(NSS)_{1-x}:Eu^{2+}$ arise from cation segregation, and microscopically, the emitting Eu^{2+} ions reside with equal probability in these domains.

Ion–ligand (lattice) interactions that split the Eu^{2+} electronic energy levels and result in spectral shifting and broadening and ion–ion interactions that promote energy transfer and change the excited-state dynamics are described in fundamental theories using similar interaction terms involving radial functions R^{-n}, where R is the distance between the RE ion and a surrounding ligand or between two RE ions and n is an integer determined by the nature of the interaction mechanism.[17,18] This basic description of the electronic interactions allows us to estimate the minimal size of the segregated domains in $(CMS)_x(NSS)_{1-x}$. According to the crystal field theory of ion–ligand interactions and Förster–Dexter theory of energy transfer (for details, see SI 1), the long-range electric dipole interaction has a distance dependence of $n = 6$. Since the distance between two lattice layers is about 0.25 nm on average, as shown in Figure 1b, cation alteration beyond 2.5 nm should have no observable effect on the RE energy levels. The same is true for the energy transfer. Numerous spectroscopic analyses and energy transfer studies of RE ions in solids have confirmed this estimation.[13,17–19] Therefore, the spectroscopic properties and decay dynamics of the photoluminescence suggest that the size of the segregated domains is 5 nm or larger.

Preliminary structural characterization using powder X-ray diffraction (PXRD) and TEM methods confirmed that an isostructural solid solution of $(CaMg)_x(NaSc)_{1-x}Si_2O_6$ is formed over the full range between the two end compounds CMS and NSS with x varied from 1 to 0.[6] In the compositionally mixed solid solution, PXRD peaks were indexed by a monoclinic cell ($C2/c$) with lattice parameters between those of $CaMgSi_2O_6$ and $NaScSi_2O_6$. The structural data and analyses are reported in the Supporting Information (SI 2). Energy-dispersive spectroscopy (EDS) mapping of a single grain using non-probe-corrected STEM showed that Ca, Na, Mg, and Sc are uniformly present within individual grains of $(CaMg)_{0.3}(NaSc)_{0.7}Si_2O_6$. However, EDS mapping at this resolution does not reveal phase segregation on the nanometer length scale. High-angle annular dark-field (HAADF) STEM, which is capable of atomic-scale resolution and provides contrast based on the local composition (average Z), was used to study the nanoscale phase segregation. On the basis of the brightness of the Z-contrast image, the darker and brighter areas in Figure 2a correspond to areas rich in Ca–Mg ($Z^2 = 544$) and areas rich in Na–Sc ($Z^2 = 562$), respectively. Such chemical segregation is further elucidated in Figure 2b, and the isostructural crystalline lattice is indicated in Figure 2c. Because the HAADF image was taken with a sample of $(CaMg)_{0.3}(NaSc)_{0.7}Si_2O_6$, there are accordingly more brighter areas than darker areas. The size of the composition-segregated domains is on the order of 5 nm, consistent with the theoretical estimate made from the spectroscopic analyses. The arrangement of atoms in each phase shown in Figure 2g indicates that the intensity profile of a Z-contrast image along the (001) plane (the red dotted line) should consist of alternating brighter and darker dots. CMS and NSS should have a reversed sequence of brightness, i.e., Ca ($Z = 20$) columns are brighter than Mg ($Z = 12$) columns for CMS and Na ($Z = 11$) columns are darker than Sc ($Z = 21$) columns for NSS. Figure 2h shows an intensity profile from the line in Figure 2d (in the (001) plane) across the darker domain. Although we did not observe perfect matching of the intensity profile reversals with those predicted for pure segregation, except in the middle of the darker domain (indicated by two red arrows in Figure 2h), there exist darker columns in the

DOI: 10.1021/jacs.5b12788
J. Am. Chem. Soc. 2016, 138, 1158–1161

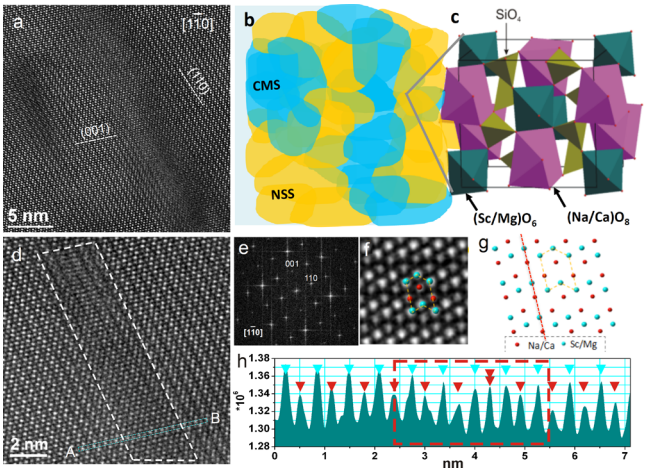

Figure 2. (a) HAADF image along [1$\bar{1}$0] zones showing nanoscale domains with different contrast. (b, c) Schematic elucidation of the segregated phases $NaScSi_2O_6$ (NSS) and $CaMgSi_2O_6$ (CMS) and their isostructural lattice. (d) Enlarged HAADF image showing that the intensities of the Sc/Mg and Na/Ca sites are similar inside the box but that the Sc/Mg sites are brighter outside of box. (e) Fourier transform of (d). (f) Enlarged HAADF image showing the experimental atomic arrangements and (g) corresponding schematic diagram. (h) Intensity profile along the line AB in (d), showing the more uniform intensity distribution between Sc/Mg and Na/Ca sites in the boxed region.

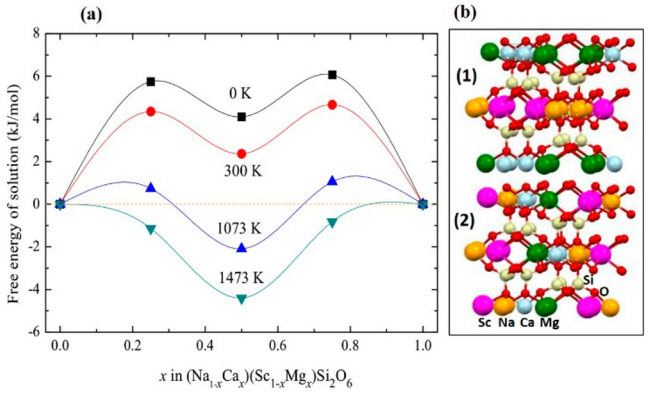

Figure 3. (a) Temperature dependence of the free energy change via DFT calculations in solid solutions of $(1-x)NaScSi_2O_6 + xCaMgSi_2O_6$ as a function of x. The solid lines are guides for the eyes. (b) The total energies calculated for various disordered composition configurations indicate that only the segregation of the Ca−Mg and Na−Sc pairs in the (200) plane (1) and along the [100] direction (2) have the lowest energy.

brighter area that gradually become brighter in the box. This observation further supports cation nanosegregation.

A comparison of the magnitudes and real parts of the EXAFS Fourier transforms (FTs) at the Ca and Sc K-edges of a compositionally mixed solid solution and the two end compounds is shown in Figure S6. The general appearance of the FTs from the Ca and Sc viewpoints are very different in the compositionally mixed solid solution and also between the end compounds themselves. This observation clearly reveals that on average Sc in the compositionally mixed solid solution has a local and medium-range structure very similar to that of Sc in NSS. The correlations at larger distances damp out for the mixed compound. This is consistent with the findings from the other techniques that strongly indicate the presence of nanoscale inhomogeneity—domains seen by STEM and optical spectroscopy and predicted by DFT (vide infra)—in an otherwise homogeneous solid solution. The overall appearance of the Ca FT in the mixed oxide has some similarity to that in CMS. In short, the EXAFS results are largely consistent with the presence of nanoscale inhomogeneity, with the medium-range structures of these nanoscale regions being quite similar to those in the end compounds.

We also investigated the energetics of the solid-solution phase of $(1-x)$NSS + xCMS using first-principles density functional theory (DFT) calculations. The calculated lattice parameters of the end members (i.e., NSS and CMS) agree well with those from experimental measurements, with relative errors less than 0.5%. The predicted lattice constants of the solution phases follow Vegard's rule, consistent with our PXRD study of the solid-solution phase (Figure S7). To evaluate the thermodynamic stability of the solution phase, the energy of solution was evaluated as follows:

$$\Delta E_{sol} = E_{tot}[(Na_{1-x}Ca_x)(Sc_{1-x}Mg_x)Si_2O_6] - (1-x)E_{tot}[NSS] - xE_{tot}[CMS] \quad (2)$$

where $E_{tot}[(Na_{1-x}Ca_x)(Sc_{1-x}Mg_x)Si_2O_6]$, $E_{tot}[NSS]$, and $E_{tot}[CMS]$ are the total energies of the solid-solution phase and its end members NSS and CMS, respectively. As shown in Figure 3, the calculated energy of solution at 0 K is positive over the whole concentration range $(0 < x < 1)$, which means that the solid-solution phases of $Na_{1-x}Ca_xSc_{1-x}Mg_xSi_2O_6$ are not thermodynamically stable at zero temperature. However, the solid-solution phase is prepared at relatively high temperatures of 1200 °C or higher. Therefore, the phase stability of the solid solution at finite temperature should be determined by the free energy change instead of the internal energy change. By including the configurational entropy contribution $T[x\ln(x) - (1-x)\ln(1-x)]$, we obtained the temperature dependence of the free energy change. At 1200 °C, the free energy of solution is negative over a wide concentration range $(0.2 < x < 0.85)$, indicating that the solid-solution phase is thermodynamically stable at high temperatures. However, the free energy of solution increases as the temperature decreases and becomes positive at room temperature, suggesting that it becomes energetically favorable for the solution phase prepared at high temperature to segregate into individual phases, which may occur as the solid solution slowly cools (via a continuous pathway from 1200 to 50 °C in 12 h). Previous reports also showed that pyroxene/pyroxene exsolution is in fact extremely common.[10,20] A continuous exsolution mechanism (spinodal decomposition) might be possible for the formation of the CMS and NSS nanosegregation mentioned above.[9,21]

In order to elucidate the tendency for phase segregation in the solid solution, the total energies of $(CaMg)_{0.5}(NaSc)_{0.5}Si_2O_6$ were calculated for various atomic configurations in which the four cations Ca, Mg, Na, and Sc are arranged differently. The calculations showed that the two configurations depicted as (1) and (2) in Figure 3b have the lowest energies. In configuration (1), the polyhedra of both $CaMgSi_2O_6$ and $NaScSi_2O_6$ occupy, respectively, the same (200) plane. In configuration (2), layers of $CaMgSi_2O_6$ and $NaScSi_2O_6$ form along the [100] direction. The minimization of energy as a result of these types of segregation would lead to the formation of layers of crystalline structures similar to those observed in the STEM image shown in Figure 2d. The energies of other configurations involving exchanges

DOI: 10.1021/jacs.5b12788
J. Am. Chem. Soc. 2016, 138, 1158−1161

between Ca and Na or between Mg and Sc are about 7 kJ/mol per formula unit higher than that of the configurations (1) and (2). The increase in the total energy for such types of cation exchanges can be understood on the basis of charge balance. These types of cation exchanges have little effect on the overall structure but lead to significant charge redistribution. Specifically, cation exchanges between (CaMg) and (NaSc) pairs are electrostatically highly unstable. The calculated results fully support the conclusions drawn from the spectroscopic analyses and HAADF imaging. From the perspective of thermodynamics, our calculations provide a potential explanation of the phase segregation in $(CaMg)_x(NaSc)_{1-x}Si_2O_6$. Microscale phase separation is not observed, and the phase separation is limited to the nanoscale. Perhaps the grain coarsening kinetics are not sufficient to allow complete microscale phase separation, limiting the segregation to the nanoscale. Such a process is dominated by spinodal decomposition, which differs from nucleation and growth in that it proceeds from a compositional perturbation that is small in degree but large in extent.[22]

In summary, the spectroscopic characteristics of Eu^{2+} demonstrated isotropic luminescence with two unique, independent spectroscopic signatures. Variation of the chemical composition, viz., the CaMg:NaSc ratio, does not perturb the electronic environment of Eu^{2+} at the two centers significantly but does change the ratio of Eu^{2+} ions at the two centers. Cation segregation via spinodal decomposition and formation of the CMS:Eu^{2+} and NSS:Eu^{2+} nanodomains in the solid solution has significant advantages for tuning of photoluminescence compared with a physical mixture or codoping of different ions.[23] First, the two emission bands are spectroscopically independent of composition variation. This dual-center solid-solution phosphor outperforms other structure- and composition-modified phosphors in which optical centers are randomly distributed in a structurally disordered lattice and both the spectral profile and luminescence intensities are unpredictable. Second, isolation of the two luminescent centers in different crystalline domains would potentially improve the light conversion efficiency since energy transfer between the two centers is limited and the largely unperturbed long-range average crystalline lattice would reduce energy lost to defects. The remarkable spectroscopic properties of the Eu^{2+}-doped $(CaMg)_x(NaSc)_{1-x}Si_2O_6$ are an example of advances in controlled photoluminescence tuning.

■ ASSOCIATED CONTENT

Supporting Information

The Supporting Information is available free of charge on the ACS Publications website at DOI: 10.1021/jacs.5b12788.

Experimental details, luminescence dynamics and theoretical models for characterization of nanosegregation, and structural, TEM and EXAFS characterization analysis (PDF)

■ AUTHOR INFORMATION

Corresponding Authors

*xiazg@ustb.edu.cn
*gkliu@anl.gov
*krp@northwestern.edu

Notes

The authors declare no competing financial interest.

■ ACKNOWLEDGMENTS

Work performed by Z.X. and Q.L. was supported by the National Natural Science Foundation of China (51272242 and 51572023), the Program for New Century Excellent Talents in the University of the Ministry of Education of China (NCET-12-0950), and the Beijing Nova Program (Z131103000413047). Work performed by G.L., J.W., Z.M., M.B., and D.J.M. at Argonne National Laboratory was supported by the Office of Basic Energy Sciences of the U.S. Department of Energy (DOE) through Grant DE-AC02-06CH11357 for research on heavy-elements chemistry and materials sciences. TEM was accomplished in part at the Center for Nanoscale Materials, a DOE Office of Science User Facility under Contract DE-AC02-06CH11357. Sector 20 operations at APS are supported by DOE and the Canadian Light Source, with additional support from the University of Washington. G.L. acknowledges travel support from the CAS/SAFEA International Partnership Program for Creative Research Teams. K.R.P. gratefully acknowledges support from the National Science Foundation (DMR-1307698).

■ REFERENCES

(1) Wang, G. F.; Peng, Q.; Li, Y. D. *Acc. Chem. Res.* **2011**, *44*, 322−332.
(2) George, N. C.; Denault, K. A.; Seshadri, R. *Annu. Rev. Mater. Res.* **2013**, *43*, 481−501.
(3) Wang, S. S.; Chen, W. T.; Li, Y.; Wang, J.; Sheu, H. S.; Liu, R. S. *J. Am. Chem. Soc.* **2013**, *135*, 12504−12507.
(4) Xia, Z. G.; Ma, C. G.; Molokeev, M. S.; Liu, Q. L.; Rickert, K.; Poeppelmeier, K. R. *J. Am. Chem. Soc.* **2015**, *137*, 12494−12497.
(5) Liu, G. K. Electronic Energy Level Structure. In *Spectroscopic Properties of Rare Earths in Optical Materials*; Liu, G. K., Jacquier, B., Eds.; Springer: Berlin, 2005.
(6) Xia, Z. G.; Zhang, Y. Y.; Molokeev, M. S.; Atuchin, V. V.; Luo, Y. *Sci. Rep.* **2013**, *3*, 3310.
(7) Mellini, M.; Merlino, S.; Orlandi, P. *Am. Mineral.* **1982**, *67*, 599−603.
(8) Merlino, S.; Orlandi, P. *Period. Mineral.* **2006**, *75*, 189−194.
(9) Cahn, J. W. *Acta Metall.* **1961**, *9*, 795−801.
(10) Jantzen, C. M. *Am. Mineral.* **1984**, *69*, 277−282.
(11) Shibata, N.; Pennycook, S. J.; Gosnell, T. R.; Painter, G. S.; Shelton, W. A.; Becher, P. F. *Nature* **2004**, *428*, 730−733.
(12) Lee, W.; Han, J. W.; Chen, Y.; Cai, Z. H.; Yildiz, B. *J. Am. Chem. Soc.* **2013**, *135*, 7909−7925.
(13) Liu, G. K. *Chem. Soc. Rev.* **2015**, *44*, 1635−1652.
(14) Inokuti, M.; Hirayama, F. *J. Chem. Phys.* **1965**, *43*, 1978−1989.
(15) Yen, W. M. *Spectroscopy of Solids Containing Rare Earth Ions*; North-Holland: Amsterdam, 1987.
(16) Liu, G. K.; Zhuang, H. Z.; Chen, X. Y. *Nano Lett.* **2002**, *2*, 535−539.
(17) Chen, X. Y.; Zhuang, H. Z.; Liu, G. K.; Li, S.; Niedbala, R. S. *J. Appl. Phys.* **2003**, *94*, 5559−5565.
(18) Newman, D. J.; Ng, B. Superposition Model. In *Crystal Field Handbook*; Newman, D. J., Ng, B, Eds.; Cambridge University Press: Cambridge, U.K., 2000.
(19) Meltzer, R. S.; Feofilov, S. P.; Tissue, B.; Yuan, H. B. *Phys. Rev. B: Condens. Matter Mater. Phys.* **1999**, *60*, R14012−R14015.
(20) Carpenter, M. A. *Contrib. Mineral. Petrol.* **1980**, *71*, 289−300.
(21) McCallister, R. H. *Contrib. Mineral. Petrol.* **1978**, *65*, 327−331.
(22) Yund, R. A.; McCallister, R. H. *Chem. Geol.* **1970**, *6*, 5−30.
(23) Shang, M.; Li, C.; Lin, J. *Chem. Soc. Rev.* **2014**, *43*, 1372.

DOI: 10.1021/jacs.5b12788
J. Am. Chem. Soc. 2016, 138, 1158−1161